Current Research in Microbial Sciences 8 (2025) 100369

Contents lists available at ScienceDirect

Current Research in Microbial Sciences

journal homepage: www.sciencedirect.com/journal/current-research-in-microbial-sciences

Quantitative multiplexed analysis of gene and protein expression patterns in *Yarrowia lipolytica*

Erin Bredeweg, Galya Orr, Dehong Hu *

Environmental Molecular Sciences Laboratory, Pacific Northwest National Laboratory, Richland, Washington 99354, USA

ARTICLE INFO

Keywords:
Yarrowia lipolytica
Fluorescence *in situ* hybridization
Single-cell
Single-molecule microscopy
Quiescence
Lipid metabolism

ABSTRACT

In this report, we present coordinated observations of protein and mRNA transcript counts at the single-cell level in the oleaginous yeast model *Yarrowia lipolytica*. The transcription factor Xbp1p regulates entry into a quiescent state, representing a shift of resources to sequestration of nutrients rather than cell division. We observed the responses of wild-type and Δ*xbp1* cells to protein (by fluorescence) and transcript quantification and localization at both single-cell and population-averaged levels. Data were collected via single-molecule fluorescence *in situ* hybridization (smFISH) and qPCR under nitrogen depletion, a condition that drives lipid accumulation. These techniques reveal a complex and heterogeneous population of Xbp1p dynamics and downstream regulation. Our findings highlight the need for single-cell resolution analyses to describe cellular dynamics and regulatory processes.

1. Background

Metabolic and regulatory pathways depend on spatial and temporal expression patterns under diverse conditions, information that is often overlooked in global omics analyses of cell populations. Predictive modeling and cell metabolism engineering would benefit from uncovering variability in pathway parameters across genetically identical cells. Unlike population averages, single-cell protein and mRNA expression values provide high-resolution cellular ranges to guide model parameters for predicting specific phenotypes. Here, we perform quantitative mapping of multiple gene and protein expression patterns to reveal spatial and temporal regulatory patterns in *Yarrowia lipolytica* cells, which are genetically identical but present different expression phenotypes.

The transcription factor Xbp1p controls uniform arrest of *Saccharomyces cerevisiae* in the G1 phase of the cell cycle, with functions that also support cell thermotolerance and longevity (Miles et al., 2013). Xbp1p acts as a repressor to halt the transcription of up to 15 % of the *S. cerevisiae* genome and is highly induced in response to glucose or nitrogen limitation (Miles et al., 2013, Miled et al., 2001). Xbp1p causes G1 cell cycle arrest by repressing cyclin cln3 transcription and binds to the promoters of other cyclins, such as cys3 and smf2 (STRING Network, 2024). Additionally, Xbp1p has genetic interactions with mitochondrial genes in *S. cerevisiae* (XBP1 BioGRID, 2025), including FMP22, F1F0 ATP synthase, GON1, MGM9, PHB2, GON5, and TIM22. Mitochondrial energy production and TCA cycle activities are directly related to quiescence and energy storage during lipid accumulation. Therefore, XBP1 mRNA or protein accumulation serves as a quiescence switch control target, with the detection of other regulated genes facilitating sensitive quantitative tracking of stationary-phase lipid metabolism. While individual gene regulation is not restricted to one transcriptional regulator, environmental conditions such as nitrogen availability shift the degree of influence of Xbp1p regulation. This work aims to clarify the multilevel regulation (mRNA and protein) that occurs during quiescence.

Many emerging spatial transcriptomics and single-cell transcriptomics technologies (Aldridge and Teichmann, 2020) involve transcript or probe amplification, increasing sensitivity but also uncertainty and making the data less quantitative. Detecting low-abundance transcripts at the single-cell level, especially in smaller cells such as microbes, is challenging for sequencing technologies. Fluorescence *in situ* hybridization (FISH) uses fluorescence probes to target nucleic acid sequences with high specificity and sensitivity (Femino et al., 1998, Raj et al., 2008), allowing sensitive and accurate quantification of mRNA copies in cells while retaining spatial information. Some FISH-related technologies, such as catalyzed reporter deposition fluorescence *in situ* hybridization (CARD-FISH), (Pernthaler and Pernthaler, 2007) are very sensitive in detecting mRNA. However, they also involve amplification,

* Corresponding author.
E-mail address: dehong.hu@pnnl.gov (D. Hu).

https://doi.org/10.1016/j.crmicr.2025.100369
Received 13 January 2025; Received in revised form 18 February 2025; Accepted 28 February 2025
Available online 2 March 2025

which makes detection less quantitative. Single-molecule FISH is frequently applied in mammalian cells and tissues, but there are fewer examples in microbial systems such as bacterial cells (Skinner et al., 2013) or fungi. (Trcek et al., 2012, Li and Neuert, 2019, Bartholomai et al., 2021) The challenge of single-molecule FISH is that the fluorescence background of cells competes with the weak fluorescence signal from FISH probes at the single-molecule level. To increase the fluorescence signal level, the number of FISH probes (Raj et al., 2008) and the number of fluorescent dye molecules per mRNA are often increased (Wang et al., 2012, Schwarzkopf et al., 2021). We discovered that the blinking of single molecules is an alternative way to improve the signal-to-background ratio for accurate counting of mRNA copies, which we term fluctuation localization imaging-based fluorescence *in situ* hybridization (fliFISH). (Cui et al., 2018) As the cells are intact, other analysis techniques can be applied to the same cell, such as observation of corresponding proteins. Here, we applied single-molecule FISH technology to quantify gene transcription in conjunction with protein translation at the single-cell level. (Miles et al., 2013, Pomraning et al., 2018)

While the expression of a few genes has been recently quantified simultaneously in budding yeast cells via single-molecule fluorescence in hybridization (FISH) (Li and Neuert, 2019, Trcek et al., 2012, Sun et al., 2020), multiplexing or barcoding for the quantitative analysis of multiple transcripts with corresponding protein expression has not been previously demonstrated in a yeast.

This work quantifies cell–to-cell variation within a population of fungal cells with distinct expression profiles not captured in bulk quantification.

Our hypothesis was that Xbp1p-based repression in *Yarrowia lipolytica* could be linked to lipid modification, parallelling regulation during quiescence in *S. cerevisiae*.[1] This finding was supported by observing Xbp1p expression via a GFP-fused protein under nitrogen limitation. To explore the link between quiescence establishment and lipid accumulation in *Y. lipolytica,* we tracked the transcriptional repressor gene XBP1 (YALI0F16511g), which is orthologous to *S. cerevisiae* XBP1. The potential for *Y. lipolytica* Xbp1p to alter lipid biosynthesis and degradation pathways in response to environmental cues such as low nitrogen could alter bioproduction approaches. The emergence of blinking probe quantification by fliFISH (Cui et al., 2018) in *Yarrowia lipolytica* combined with monitoring protein expression strength by fluorescence allows the assessment of variable phenotypes at multiple levels of regulation.

2. Methods

2.1. Growth and maintenance of Yarrowia lipolytica strains

Five strains of *Yarrowia lipolytica* were used for this work. These strains include a prototrophic 'wild type' (wt, FKP391) (Bredeweg et al., 2017), an XBP1, YALI0F16511g deletion strain (Δ*xbp1*, FEB272), and the GFP transcriptional fusions XBP1-GFP (FEB738), TGL1-GFP (FEB741), and ELO2-GFP (FEB744). The strains were maintained as -80 C stocks in 25 % glycerol (see Table S4). They were subsequently grown in YPD media (10 g/L yeast extract (Fluka), 10 g/L bacto-peptone (BD), and 20 g/L glucose) at 28 °C for 24 h, followed by transfer to fresh YPD or YPD without peptone.

2.2. Strain construction for fluorescent tagged proteins and gene knockout

The Δ*xbp1* mutant and the XBP1-, TGL1-, and ELO2-GFP strains presented altered genomic locations via homologous recombination. Integration homology arms were PCR amplified (see primer table S2) from genomic DNA and fused to the ura3 marker via overlap PCR (Bredeweg et al., 2017) (see Figure S1). The resulting DNA was transformed into FEB 130 (matA, *xpr2*-332, *Δaxp-2, Δku70*::hph+, *leu2*-270::LEU2+, *ura3*-) (**Table S4**) via a PEG and heat shock transformation procedure. Colonies were isolated, prepped for DNA (MasterPure) and confirmed via PCR (see Table S1) by amplification for the presence/absence of altered DNA, as well as screening for localized GFP signals.

2.3. Yarrowia lipolytica experimental culture preparation

Briefly, 10 mL of YPD was inoculated with FKP 391, FEB 272, or FEB 738 (Table S4). These cultures were grown overnight before being harvested at t=0 h. Samples were taken for RNA extraction, and separate aliquots were subjected to light fixation for FISH preparation and analysis (RNA pellet: 1 mL; FISH: 500 μL). For each purpose, a volume of culture was spun down at 1000 rcf for 1 min, and the spent media was removed. For RNA extraction, the cell pellets were frozen until RNA extraction (YeaSTAR RNA Kit, Zymo Research). For FISH, a solution of 4% PFA in PBS was added, and the resulting pellet was resuspended. After 20 min of incubation at room temperature, the cells were again spun at 1000 rcf and washed 2 times with PBS before being stored at -20 °C in a 50 % PBS and 50 % ethanol mixture prior to FISH. The remaining 8 mL of culture was spun down in a 15 mL conical, washed once in YNB without N and resuspended in YNB media (1.7 g/L YNB salts, 20 g/L glucose and autoclaved for 20 min at 121 °C to sterilize) with no nitrogen component, conditions used for stimulating lipid accumulation. Samples were taken in the same manner at 1 h, 4 h and 24 h after media transfer for both RNA extraction and FISH.

2.4. FISH probe sequence design

Three genes were selected for this study. They are ELO2 (YALI0B20196g), TGL1 (YALI0E32035g), and XBP1 (YALI0F16511g). Along their mRNA sequences, multiple segments were selected as FISH targets. The locations of FISH targets on mRNA sequences are illustrated in Fig. 1. The FISH probe sequences are summarized in Table S2 of the supplementary material. The FISH probes were designed on the basis of the published concept (Tsanov et al., 2016) of primary and secondary FISH probes. The primary probes contain a target mRNA transcript-binding domain and a FLAP-binding domain. The secondary probes (FLAPs) were conjugated with fluorescent dyes. Both the primary probes and dye-labeled secondary probes were purchased from Integrated DNA Technologies, Inc. (Coralville, Iowa, USA). The sequences of the primary probes' mRNA transcript-binding domain and secondary probe sequences are listed in Table S2. All the XBP1 primary probes also have a domain to match the secondary probe conjugated with Alexa750. All the ELO2 primary probes also have a domain to match the secondary probe conjugated with Alexa 647. All the primary TGL1 probes also have a domain to match the secondary probe conjugated with Alexa 594.

2.5. Fluorescence in situ hybridization procedure

The cells stored in 50 % ethanol in 50 % PBS were washed with 1.2 M sorbitol in PBS with 0.02 % SDS. The cells were subsequently incubated in 1.2 M sorbitol in PBS, 20 mM ribonucleoside vanadyl complexes, 0.2 % beta-mercaptoethanol, and 0.5 mg/ml lyticase (Sigma, L4025) for 30 min at 30 °C in a hybridization oven (Boekel Bambino) for cell wall permeabilization. After permeabilization, the cells were washed twice with wash buffer (0.04 M Tris, 1 mM EDTA, 0.01 % SDS, 0.9 M NaCl). For hybridization, the cells were incubated with 20 % formamide (v/v), 0.9 M NaCl, 0.02 M Tris, 0.01 % SDS, and 1 mg/ml tRNA (Roche 10109541001), and FISH probes were synthesized overnight in a hybridization oven at 46 °C. After hybridization, the cells were washed with wash buffer twice, each 15 min at 46 °C. Then, the cells were further washed with PBS buffer and kept in PBS buffer until imaging.

2.6. Fluorescence microscopy image acquisition and data processing

For GFP expression localization in YPD and YD (low nitrogen) media,

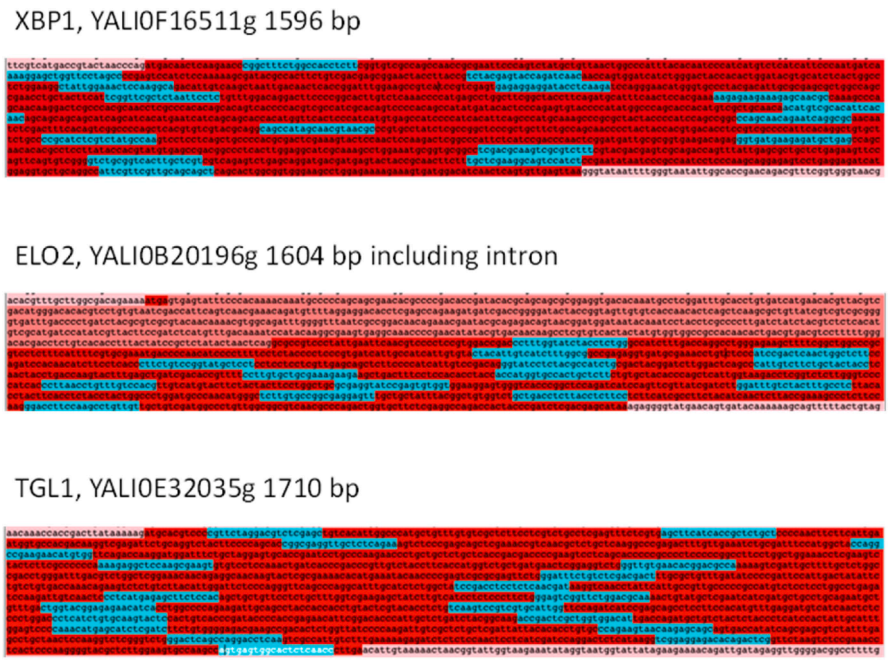

Fig. 1. mRNA probe maps of XBP1, ELO2, and TGL1. pink: genome sequence; dark pink: intron; red: gene sequence; teal: probe sequences.

the cells were imaged on a Zeiss LSM710 confocal microscope using a 488 nm laser. Approximately 5 μl of cells were dropped in their respective media on a microscope slide and imaged using immersol and a 100X oil lens. For single-molecule FISH and correlated GFP fluorescence detection, cells in the buffer were dropped on polylysine-coated microscope coverslips. The buffer solution on the coverslip was 10 mM Tris buffer, 10 % glucose, 0.5 mg/ml glucose oxidase, and 0.12 mg/ml catalase. Another coverslip was then placed on the top. The edge was sealed with nail polish. The cells on coverslips were imaged with an Olympus IX71 microscope with a 100 × oil lens and an Andor EMCCD iXon 897 camera. The setup of the microscope and data acquisition process were published previously. (Cui et al., 2018) The samples were sequentially imaged via brightfield microscopy at 488 nm excitation wavelengths for GFP and at 730 nm, 642 nm, and 594 nm excitation wavelengths for single-molecule FISH. The procedure of identifying single mRNA transcripts from blinking single-molecule fluorescence in microbes was published previously (Hu et al., 2021). The cell size was measured via the AI-enabled image segmentation software CellPose (Pachitariu and Stringer, 2022) from the bright field images.

2.7. RNA extraction from Yarrowia lipolytica

RNA was extracted from frozen cell pellets, following the protocol for the YeaSTAR kit as described previously, via vigorous vortexing with glass beads in lieu of a bead beater. The pellet suspensions were incubated for 1 hour at 37 °C in a water bath in Zymolyase solution. Ethanol addition postincubation was performed in proportion to the full volume of existing lysate from the kit instructions. The samples were eluted in 60 μl of nuclease-free water and stored at -20 °C. Prior to cDNA analysis by RT−qPCR, the extracts were treated with DNase I (NEB) and purified via LiCl for precipitation.

2.8. qPCR analysis of mRNA transcript levels

cDNA was generated via the ProtoScript II kit (NEB), with a 1:10 representation of random hexamers (0.2 μL) and oligo-dT primers (1.8 μl) for the conversion reaction. For each reaction, the input RNA was normalized to 400 ng. For RT−qPCR, 1 μl of the resulting mixture was added to each well. The primers and probes (IDT, with ZEN and FAM, see Table S3) were diluted to 100 μM in sterile water before the reaction components were extracted and run on an Applied Biosystems 7500 RT−qPCR system under standard cycling conditions: 3 min. 95 °C; 49 × (15 s. 95 °C; 1 min. 60 °C) and ROX reference dye at a 'low' concentration. Sec62 was used as a housekeeping gene for expression normalization. (Borkowska et al., 2020) The qPCR primers and probes used are listed in Table S3.

3. Results

To track the regulatory responses of XBP1 (gene) and Xbp1p (protein) to nutrient conditions, we first undertook live-cell observations of GFP-tagged Xbp1p and lipid-interacting enzymes (elongase Elo2p and lipase Tgl1p) in *Yarrowia lipolytica*. Figure 2 Confocal fluorescence microscopy images demonstrating the responsiveness of the *Yarrowia* Xbp1p and Xbp1p-regulated genes in response to changing nitrogen levels. Xbp1p signals were observed in the nucleus after 24 h in yeast extract-dextrose without peptone. Similarly, Tgl1p expression intensifies at the lipid droplet periphery in low-nitrogen media, and Elo1p expression at the ER in YPD becomes more generalized to the plasma membrane. Notably, there is population heterogeneity among these patterns, with cell size and expression level varying across the population. Our data capture a higher resolution of protein and mRNA regulation in a non-synchronized population, indicating that this technique can uncover dependencies obscured by population trends.

As this preliminary protein localization study via confocal microscopy revealed responses to environmental changes, we thoroughly investigated gene expression and translation via single-molecule fluorescence in hybridization (FISH) at the single-cell level. Three strains of Yarrowia (wt, Δ*xbp1*, and Xbp1p-GFP) were imaged at two time points, 0 h and 24 h, in low-nitrogen media. At least 50 cells per strain per time point were imaged. Each cell provided data on the mRNA counts of XBP1, ELO2, and TGL1. For the Xbp1p-GFP cells, the GFP fluorescence intensity was also acquired, and the cell size was measured from bright field images. The full datasets of mRNA counts, fluorescence intensity and cell size are in Excel file Data Set 1 in the supplementary materials. The data were analyzed at the single-cell level, and their average values were compared with those of qPCR (Fig. 5). Because single-molecule FISH measurements at the single-cell level are very time consuming,

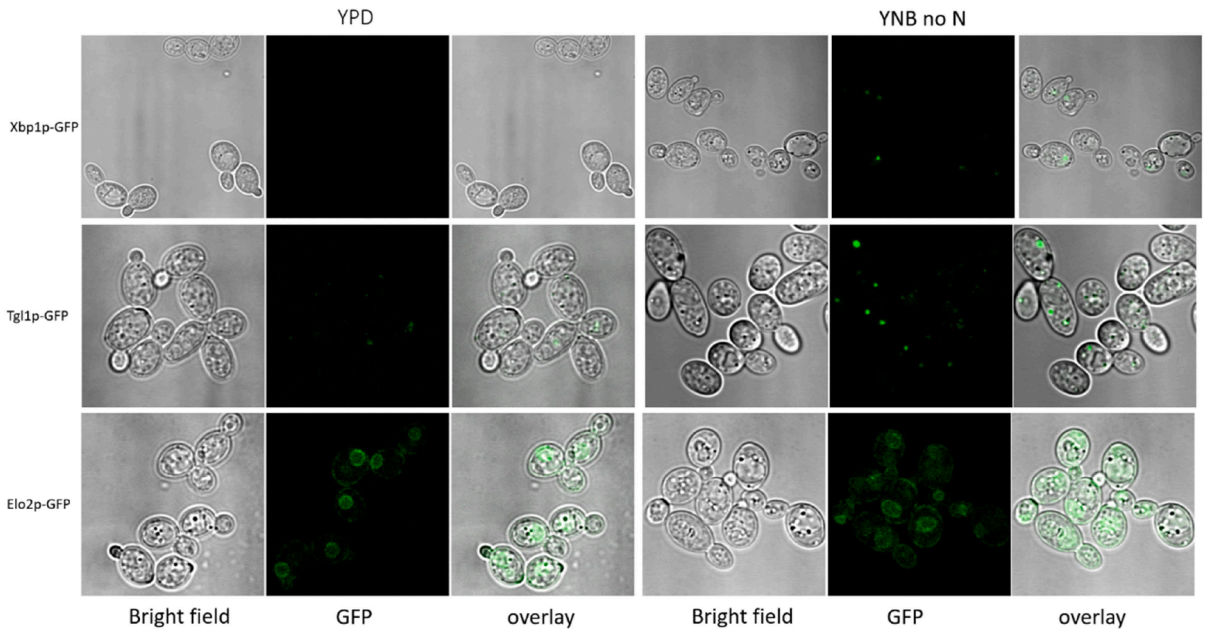

Fig. 2. *Yarrowia lipolytica* confocal microscopy. Images of endogenously tagged GFP to track proteins of interest. Xbp1p-regulated conditions of a switch from normal to low-nitrogen conditions display altered expression and localization of Xbp1p-GFP, Tgl1p-GFP, and Elo2p-GFP.

experiments were conducted only on representative strains at representative time points.

We analyzed the transcript counts of the Δ*xbp1* strain in the same way that the transcripts of the other strains were analyzed as a control. Due to autofluorescence, there is a small chance of false positive identification of transcripts. We found that the average copy number of XBP1 transcript per cell in the Δ*xbp1* strain from our analysis was 1, which was set as our measurement baseline. The XBP1, TGL1 and ELO2 mRNA copies per cell in actual studies are in the tens, making the 1-count baseline insignificant.

After 24 h in low-nitrogen medium, the cells underwent significant morphological changes, as shown by bright-field microscopy images. (See Fig. 3 for bright-field images.) Xbp1p, which plays a crucial role in regulating cell growth and is considered a transcriptional repressor, is not expressed during the log phase of growth but is induced by nutrient stress. Our Xbp1p-GFP strain showed that at 0 h, Xbp1p protein expression was low and not visible, whereas at 24 h, the Xbp1p protein was in the nucleus region of the cells. Fig. 3 displays typical wide-field fluorescence images of cells at 0 and 24 h, which are consistent with the confocal images in Fig. 2. At 0 h, the cells exhibited a diffuse, weak background level of fluorescence in the GFP channel. At 24 h, bright fluorescent spots appeared in the cell nucleus region. Although the fluorescence intensity of GFP does not translate to the absolute copy number of GFP molecules, the fluorescence intensity of these spots provides a relative representation of the amount of the Xbp1p protein present in the cell. Fig. 4D shows the fluorescence intensity of Xbp1p-GFP at 24 h in low-nitrogen medium in single cells versus transcript copy number. The fluorescence intensity of Xbp1p-GFP varied across cells at 24 h, indicating a wide distribution. (Fig. 4D, vertical axis). This variation indicates that cell responses to environmental changes are heterogeneous across a cell population, underscoring the importance of measuring biological processes at the single-cell level. Possible reasons for differences in Xbp1p protein levels include variable mRNA transcription in response to environmental changes or cells being at different ages or growth stages when the environment changes.

To further investigate the cell signaling process involving Xbp1p, we analyzed the mRNA transcripts at single-cell resolution. The average number of XBP1 mRNA transcripts was greater in the wild-type cells at 24 h than at 0 h. (Fig. 4A or B, horizontal axis, blue vs orange dots).

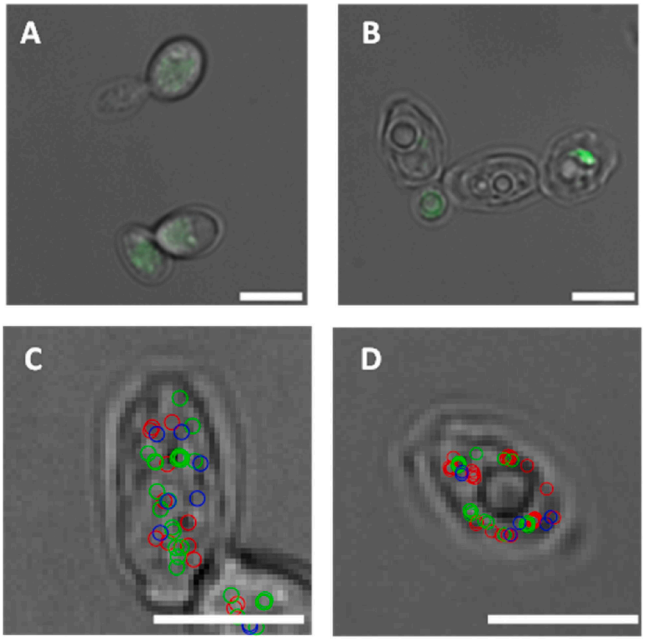

Fig. 3. Examples of single-cell images. (A) and (B) Green fluorescence overlay with bright field (gray) images of the Xbp1p-GFP strain at 0 h (A) and 24 h (B). (C) and (D) bright field images of wild-type strains at 0 h (C) and 24 h (D). The red, green and blue cycles indicate the locations of the identified transcripts XBP1, ELO2, and TGL1, respectively. The scale bar is 5 μm.

These findings are consistent with the qPCR data (Fig. 5). However, the number of XBP1 mRNA transcripts per cell varies widely. (Fig. 4A and B, horizontal axis). At 0 h, the average XBP1 transcript level per cell was 18, with a standard deviation of 17. At 24 h, the average XBP1 transcript level per cell was 56, with a standard deviation of 31. The Xbp1p-GFP strain presented the same trend, where the XBP1 transcript was more abundant at 24 h than at 0 h. At the single-cell level, XBP1 expression has a broad distribution. In summary, after 24 h of nitrogen deprivation, the cells produced more XBP1 mRNA transcripts and expressed more

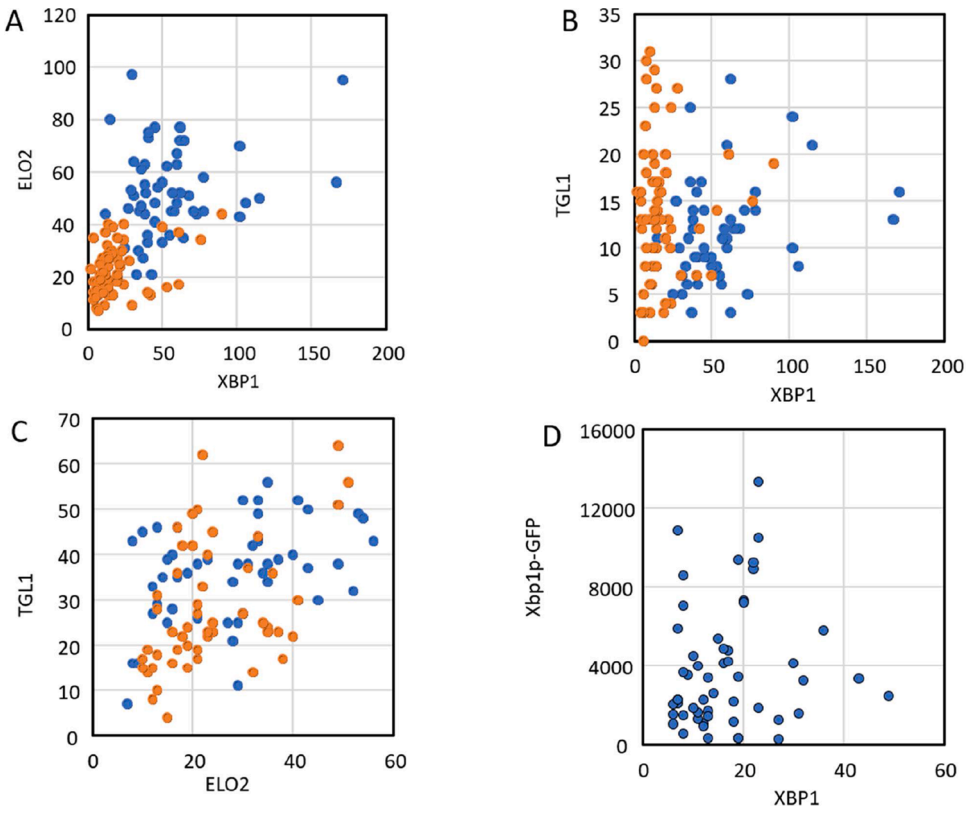

Fig. 4. Single-cell mRNA transcript counts and protein expression levels. (A) ELO2 mRNA counts vs. XBP1 mRNA counts of wild-type cells. (B) tgl1 mRNA counts vs. xbp1 mRNA counts of wild-type cells. (C) TGL1 mRNA counts vs ELO2 mRNA counts of *Δxbp1* cells. (D) GFP fluorescence intensity vs. XBP1 mRNA count of the Xbp1p-GFP strain. The orange and blue dots represent cells at 0 h and 24 h of nitrogen deprivation, respectively.

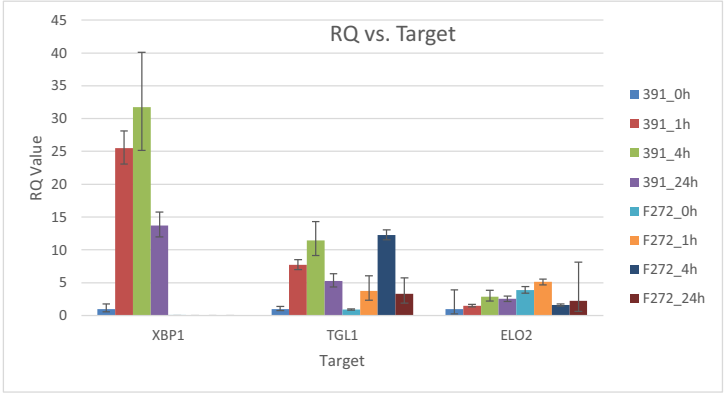

Fig. 5. Population-level qPCR of transcripts from samples collected in parallel with fliFISH data comparing the expression of lipid-related enzyme targets in the wild-type and dxbp1 strains. XBP1 cDNA quantification confirmed that expression was lost in FEB272. TGL1 peaks at 4 h both with and without XBP1. ELO2 was highly expressed at 0 and 1 h in FEB272, suggesting a loss of repression.

Xbp1p protein on average.

Next, we aimed to correlate the amount of the XBP1 mRNA transcript with the amount of the Xbp1p protein in the 24-hour Xbp1p-GFP cells. Population-level mRNA levels have been used as a proxy for protein levels and their cellular functions. However, single-cell experiments in mammals have revealed a gene-specific relationship between mRNAs and proteins and that direct mRNA–protein relationships are widely distributed in single cells. In *S. cerevisiae*, early work has shown that genes with low abundance have poor quantitative mRNA–protein correlations. (Gygi et al., 1999) We also observed that at the single-cell level within a cell culture, the scatter plot of protein amount vs. mRNA number in Fig. 4D did not show a significant correlation according to the Pearson correlation coefficient. The Pearson correlation coefficient is a common way of measuring the strength and direction of the linear correlation between two variables. A coefficient near 1 indicates a strong positive correlation, whereas a coefficient of 0 indicates no correlation. The Pearson correlation coefficient of the points in Fig. 4D is 0.10. It is only a very weak positive correlation. While this finding is consistent with the XBP1 mRNA and protein data for a population average comparing 24 h vs 0 h growth conditions, the single-cell data revealed more complex regulatory processes. In Fig. 4D, there are a few apparent "outlier" points describing single-cell XBP1 mRNA levels, corresponding to a few cells with very high protein expression levels or high mRNA transcript levels. We also tested whether outliers skew the data and reduce the strength of a true correlation and found that this is not the case. All the data points should be included in the statistics, and

no points should be considered outliers.

One study reported that the mRNA transcription level of fission yeast cells is related to their length. (Sun et al., 2020) Intuitively, larger cells would have higher transcription and translation levels. Therefore, we analyzed the XBP1 mRNA level and Xbp1p protein level vs. cell size. Unlike fission yeast (Sun et al., 2020), Yarrowia remains elliptical in shape under our growth conditions and does not undergo significant shape changes. The size distribution is narrower than the mRNA and protein distributions. The XBP1 mRNA level vs. cell size and the Xbp1p protein level vs. cell size are plotted in supporting information Figure S2. They do not show a significant correlation. Therefore, cell size is not a major contributing factor to single-cell transcription and translation heterogeneity.

Elo2p fatty acid elongase is an important factor related to lipid accumulation under N limitation. qPCR data (Fig. 5) revealed that in WT cells, ELO2 transcripts were more abundant at 24 h than at 0 h. The single-molecule mRNA FISH data also revealed that, on average, there were more transcripts at 24 h than at 0 h (average 53 vs. 23 transcripts per cell) (Fig. 4 vertical axis, blue vs. orange dots). At the single-cell level, ELO2 transcription has a broad distribution. As Xbp1p is considered the controlling factor of other downstream genes, such as ELO2, we analyzed the correlation of XBP1 and ELO2 transcripts at the single-cell level. For the WT at both 0 h and 24 h, the single-cell plot of XBP1 vs ELO2 showed a weak correlation (Fig. 4A). The Pearson correlation coefficients are 0.22 and 0.36 for 24 h and 0 h, respectively. The reason for the weak correlation between the ELO2 and XBP1 transcripts is similar to the weak correlation between the XBP1 transcripts and the Xbp1p protein. The timing difference among cells means that high Xbp1p does not always translate to high ELO2 mRNA counts for individual cells. Similar to Xbp1p protein vs. mRNA, at the population-wide average, a higher ELO2 mRNA count was correlated with a higher XBP1 mRNA count at 24 h vs. 0 h. The population-averaged data indicate that XBP1 is a controlling factor of ELO2. However, single-cell data reveal more complex processes than simple models in which Xbp1p controls ELO2.

Although there was only a weak correlation between the XBP1 count and ELO2 count at the single-cell level within the culture, the qPCR results and averaged FISH data revealed that XBP1 and ELO2 were correlated in response to growth medium changes. Comparison of GFP-tagged and wild-type strain FISH data with those of the Δ*xbp1* strain was performed to investigate the relationship between Xbp1p function and ELO2 expression. The qPCR results of Δ*xbp1* cells revealed no increase in ELO2 at 24 h compared with 0 h. Single-molecule FISH also revealed that, on average, ELO2 mRNA counts are not significantly greater at 24 h than at 0 h (average 28 standard deviations of 14 vs average 25 standard deviations of 11, respectively). In Δ*xbp1* cells, we plot TGL1 vs ELO2 mRNA transcript counts in single cells in Fig. 4C because we observed few or no mRNA transcript counts of XBP1. Along the horizontal axis ELO2 counts, there is no significant difference between the orange and blue dots. This result suggests that Xbp1p is a controlling factor of ELO2. Without XBP1, elo2 mRNA did not respond to the growth medium change.

The third gene of *Yarrowia* that we analyzed was TGL1. Tgl1p is a triglyceride lipase enzyme responsible for lipolysis at lipid droplets. At both 0 h and 24 h, the number of TGL1 transcripts per cell was widely distributed and was not significantly correlated with the number of XBP1 transcripts. (Fig. 4B, vertical axis). The TGL1 transcript copy numbers were 11±5 and 14 ± 7 (average ± standard deviation), respectively, at 0 h and 24 h.

4. Discussion

We observed a wide distribution of protein translation of Xbp1p and mRNA transcript levels of XBP1, ELO2 and TGL1 at the single-cell level. It is natural to ask whether the observed heterogeneity in Xbp1p-GFP translation and XBP1, ELO2 and TGL1 mRNA expression is due to biological response or experimental measurement artifacts. We have considered several factors. First, we used a genomic integration strategy to fuse the GFP coding sequence to the target protein with a short glycine linker, which was constructed via overlap PCR and verified via microscopy and qPCR. This ensures that the GFP signal reflects endogenous protein level regulation, with genomic targeting of the GFP fusion construct avoiding variability associated with plasmid numbers. Second, there are few sample processing and data processing steps for measuring GFP fluorescence intensity, resulting in few chances of data error. We used the same microscope settings for all images, such as laser power, filters, camera gain and exposure. We observed a large variation in the GFP intensity among single cells under the same growth conditions, even within the same image, indicating that the fluorescence differences are not due to experimental errors. This must be due to variations in the amount of protein present in individual cells. Third, the qPCR data and average cell transcript levels from FISH are consistent in showing the same trend of increasing/decreasing transcript levels caused by changes in growth conditions and mutations. However, we acknowledge that quantitative single-cell FISH data are difficult to validate by other methods, especially at low expression levels. Nonetheless, it is unlikely that cells have identical mRNA expression but different protein translation for the same gene. The wide distribution of mRNA transcripts in single cells is no surprise. A variety of biological systems, from microbial cells to cultured mammalian cells, also display wide variation in transcript levels (Mitchell et al., 2016, Raj et al., 2008, Taniguchi et al., 2010, Raj and van Oudenaarden, 2008). Potential explanations for mRNA–protein signal variation include delays between mRNA transcription and protein translation, offset timing of protein or mRNA persistence, cells being at different points of the cell cycle during environmental shifts, or posttranslational modifications of proteins.

The inclusion of regulatory networks in bioengineering models of lipid accumulation during nitrogen limitation will support controllable, predictable cellular behavior and morphology for industrial growth (Miles et al., 2013, Pomraning et al., 2018). In addition to regulation and morphology, omics data are used to constrain FBA models. However, transcripts may have multiple layers of regulation that we miss. Combinatorial regulation by transcription factors as well as the expression of partially functionally redundant enzymes may affect lipid profiles. Xbp1p is a transcription factor that regulates the expression of the XBP1 transcript, which affects the transcription of TGL1 and ELO2 after translation (Miles et al., 2013) in *S. cerevisiae*. In a large population of cells across different growth stages, we detected the correlation of XBP1 transcripts with Xbp1p protein expression and TGL1 and ELO2 transcript levels via both qPCR and average numbers via single-cell analysis. However, at the single-cell level, individual cells may have different responses to the conditions that modulate this transcription factor. This difference could be attributed to a spectrum of cell ages, additional regulatory protein interactions, or differing nutritional statuses. Moreover, at a specific point in observation (the time at which we fix the cell), the number of transcripts and protein molecules are influenced by the stage of cell growth and cell signaling. Therefore, these numbers vary widely and are not correlated.

Compared with population-level measurements, quantitative analysis of single-cell mRNA transcription and protein expression provides additional information about posttranslational modifications and growth stage-related gene expression. Furthermore, single-cell analysis reports individual cell phenotypes. For example, single mammalian cells take up nanoparticles differently within the same culture. The cells with higher/lower nanoparticle uptake have distinct gene expression patterns (Mitchell et al., 2016). Single-cell technologies inspire future investigations into the cell response related to growth stage and individuality.

Funding declaration

This research was performed on project award 51679 from the

Environmental Molecular Sciences Laboratory, a DOE Office of Science User Facility sponsored by the Biological and Environmental Research Program under Contract No. DE-AC05-76RL01830.

Author contributions

E. B., G. O., and D. H. conceptualized the research. E. B. Cultured the system. E. B. performed confocal microscopy. E. B. performed the qPCR. D. H. performed FISH, single-molecule microscopy and image analysis. E. B., G. O. and D. H. wrote the manuscript.

Declaration of competing interest

The authors declare no competing interests.

Acknowledgement

The authors thank Justin Teeguarden for helpful discussions.

Supplementary materials

Supplementary material associated with this article can be found, in the online version, at doi:10.1016/j.crmicr.2025.100369.

Data availability

Publicly available datasets and images were analyzed in this study. These data can be found here: https://search.emsl.pnnl.gov/?project[0]=projects_51679.

References

Aldridge, S., Teichmann, SA., 2020. Single cell transcriptomics comes of age. Nat. Commun. 11 (1), 4307. https://doi.org/10.1038/s41467-020-18158-5.

Bartholomai, B.M., Gladfelter, A.S., Loros, J.J., Dunlap, JC., 2021. Quantitative single molecule RNA-FISH and RNase-free cell wall digestion in Neurospora crassa. Fungal Genet. Biol. 156, 103615. https://doi.org/10.1016/j.fgb.2021.103615.

Borkowska, M., Białas, W., Celińska, E., 2020. A new set of reference genes for comparative gene expression analyses in Yarrowia lipolytica. FEMS. Yeast. Res. 20 (7). https://doi.org/10.1093/femsyr/foaa059.

Bredeweg, E.L., Pomraning, K.R., Dai, Z., Nielsen, J., Kerkhoven, E.J., Baker, SE., 2017. A molecular genetic toolbox for Yarrowia lipolytica. Biotechnol. Biofuels. 10 (1), 2. https://doi.org/10.1186/s13068-016-0687-7.

Cui, Y., Hu, D., Markillie, L.M., Chrisler, W.B., Gaffrey, M.J., Ansong, C., et al., 2018. Fluctuation localization imaging-based fluorescence in situ hybridization (fliFISH) for accurate detection and counting of RNA copies in single cells. Nucleic. Acids. Res. 46 (2), e7. https://doi.org/10.1093/nar/gkx874.

Femino, A.M., Fay, F.S., Fogarty, K., Singer, RH., 1998. Visualization of single RNA transcripts in situ. Science (1979) 280 (5363), 585–590. https://doi.org/10.1126/science.280.5363.585.

Gygi, S.P., Rochon, Y., Franza, B.R., 1999. Aebersold R. Correlation between protein and mRNA abundance in yeast. Mol. Cell Biol. 19 (3), 1720–1730. https://doi.org/10.1128/mcb.19.3.1720.

Hu, D., Cui, Y., Markillie, L.M., Chrisler, W.B., Wang, Q., Hatzenpichler, R., Orr, G., 2021. Counting mRNA copies in intact bacterial cells by fluctuation localization imaging-based fluorescence in situ hybridization (fliFISH). In: Azevedo, N.F., Almeida, C. (Eds.), Fluorescence In-Situ Hybridization (FISH) for Microbial Cells: Methods and Concepts. Springer US, New York, NY, pp. 237–247.

Li, G., Neuert, G., 2019. Multiplex RNA single molecule FISH of inducible mRNAs in single yeast cells. Sci. Data 6 (1), 94. https://doi.org/10.1038/s41597-019-0106-6.

Miled, C., Mann, C., Faye, G., 2001. Xbp1-mediated repression of CLB gene expression contributes to the modifications of yeast cell morphology and cell cycle seen during nitrogen-limited growth. Mol. Cell Biol. 21 (11), 3714–3724. https://doi.org/10.1128/MCB.21.11.3714-3724.2001.

Miles, S., Li, L., Davison, J., Breeden, LL., 2013. Xbp1 directs global repression of budding yeast transcription during the transition to quiescence and is important for the longevity and reversibility of the quiescent state. PLoS. Genet. 9 (10), e1003854. https://doi.org/10.1371/journal.pgen.1003854.

Mitchell, H.D., Markillie, L.M., Chrisler, W.B., Gaffrey, M.J., Hu, D., Szymanski, C.J., et al., 2016. Cells respond to distinct nanoparticle properties with multiple strategies as revealed by single-cell RNA-Seq. ACS. Nano 10 (11), 10173–10185. https://doi.org/10.1021/acsnano.6b05452.

Pachitariu, M., Stringer, C., 2022. Cellpose 2.0: how to train your own model. Nat. Methods 19 (12), 1634–1641. https://doi.org/10.1038/s41592-022-01663-4.

Pernthaler, A., Pernthaler, J., 2007. Fluorescence in situ hybridization for the identification of environmental microbes. Methods Mol. Biol. 353, 153–164. https://doi.org/10.1385/1-59745-229-7:153.

Pomraning, K.R., Bredeweg, E.L., Kerkhoven, E.J., Barry, K., Haridas, S., Hundley, H., et al., 2018. Regulation of yeast-to-hyphae transition in Yarrowia lipolytica. mSphere 3 (6). https://doi.org/10.1128/mSphere.00541-18.

Raj, A., van den Bogaard, P., Rifkin, S.A., van Oudenaarden, A., Tyagi, S., 2008. Imaging individual mRNA molecules using multiple singly labeled probes. Nat. Meth. 5 (10), 877–879. https://doi.org/10.1038/nmeth.1253.

Raj, A., van Oudenaarden, A., 2008. Nature, nurture, or chance: stochastic gene expression and its consequences. Cell 135 (2), 216–226. https://doi.org/10.1016/j.cell.2008.09.050.

Schwarzkopf, M., Liu, M.C., Schulte, S.J., Ives, R., Husain, N., Choi, H.M.T., Pierce, NA., 2021. Hybridization chain reaction enables a unified approach to multiplexed, quantitative, high-resolution immunohistochemistry and in situ hybridization. Development 148 (22). https://doi.org/10.1242/dev.199847.

Skinner, S.O., Sepulveda, L.A., Xu, H., Golding, I., 2013. Measuring mRNA copy number in individual Escherichia coli cells using single-molecule fluorescent in situ hybridization. Nat. Protoc. 8 (6), 1100–1113. https://doi.org/10.1038/nprot.2013.066.

STRING Network https://version-12-0.string-db.org/cgi/network?networkId=b4g8yfm7t95w 2024.

Sun, X.-M., Bowman, A., Priestman, M., Bertaux, F., Martinez-Segura, A., Tang, W., et al., 2020. Size-dependent increase in RNA polymerase II initiation rates mediates gene expression scaling with cell size. Curr. Biol. 30 (7), 1217–1230. https://doi.org/10.1016/j.cub.2020.01.053 e7.

Taniguchi, Y., Choi, P.J., Li, G.-W., Chen, H., Babu, M., Hearn, J., et al., 2010. Quantifying E. coli proteome and transcriptome with single-molecule sensitivity in single cells. Science (1979) 329 (5991), 533–538. https://doi.org/10.1126/science.1188308.

Trcek, T., Chao, J.A., Larson, D.R., Park, H.Y., Zenklusen, D., Shenoy, S.M., Singer, RH., 2012. Single-mRNA counting using fluorescent in situ hybridization in budding yeast. Nat. Protoc. 7, 408. https://doi.org/10.1038/nprot.2011.451.

Trcek, T., Chao, J.A., Larson, D.R., Park, H.Y., Zenklusen, D., Shenoy, S.M., Singer, RH., 2012. Single-mRNA counting using fluorescent in situ hybridization in budding yeast. Nat. Protoc. 7 (2), 408–419. https://doi.org/10.1038/nprot.2011.451.

Tsanov, N., Samacoits, A., Chouaib, R., Traboulsi, A.M., Gostan, T., Weber, C., et al., 2016. smiFISH and FISH-quant - a flexible single RNA detection approach with super-resolution capability. Nucleic. Acids. Res. 44 (22), e165. https://doi.org/10.1093/nar/gkw784.

Wang, F., Flanagan, J., Su, N., Wang, L.C., Bui, S., Nielson, A., et al., 2012. RNAscope: a novel in situ RNA analysis platform for formalin-fixed, paraffin-embedded tissues. J. Mol. Diagn. 14 (1), 22–29. https://doi.org/10.1016/j.jmoldx.2011.08.002.

XBP1 BioGRID. https://thebiogrid.org/34891/summary/saccharomyces-cerevisiae/xbp1.html 2025.